WPI

Design of an Arm Simulator for Testing Wearable Blood Pressure Monitoring Device

A Major Qualifying Project (MQP) Report
Submitted to the Faculty of
WORCESTER POLYTECHNIC INSTITUTE
in partial fulfillment of the requirements for the
Degree of Bachelor of Science in
Mechanical Engineering
Robotics Engineering
Electrical Engineering
Biomedical Engineering

Submitted By:
Michael Haroutunian
Tevin Makoye
Matheos Simantirakis
Anna Zauha

Submitted to:
Professor Yihao Zheng, Mechanical and Materials Engineering Department

Submission Date:
April 25, 2024

Table of Contents

List of Figures

List of Tables

Abstract

Nearly 119.9 million adults in the US suffer from hypertension, requiring frequent blood pressure measurements. The modern blood pressure cuff has lacked developments since its introduction. It remains a bulky design requiring high pressures and long times to achieve accurate readings. A slimmer cuff has been developed, but when tested on human subjects, has been unable to produce accurate readings compared to traditional cuffs. To help streamline the testing and advancement of the slimmer cuff technology, this project aims to design, fabricate, and validate an anatomically and physiologically representative arm simulator to enable mechanistic investigation of the cuff size effect on blood pressure measurement. The simulator consists of a tissue mimicking model, a controllable blood pressure source, and a blood pressure data acquisition system. The team developed and tested a series of designs and provided recommendations for future improvements to the system.

1.0 Introduction

1.1 Problem and Goal

Nearly 119.9 million adults in the United States, equivalent to roughly half of the population, suffer from hypertension, defined as an elevated blood pressure with systolic pressure greater than 130 mmHg and diastolic pressure greater than 80 mmHg (Centers for Disease Control and Prevention, 2023). As a result of the elevated blood pressures, frequent blood pressure measurements are required to monitor the disease. The modern blood pressure cuff has not undergone many advancements or redesigns since its implementation in 1901 (Rader and Victor, 2017). In its current design, the cuff is bulky and requires high pressure levels for accurate readings, making the process uncomfortable and cumbersome for patients. A previous group of researchers developed a smaller cuff design but were unable to produce accurate readings compared to the existing blood pressure cuff when tested on human subjects. The goal of this project was to help streamline the testing and advancement of the slim cuff technology by designing, fabricating, and validating an anatomically and physiologically representative arm simulator that can be used in future research for the redesign of the blood pressure cuff that has a smaller cuff profile, requires less pressure, and provides consistently accurate readings. This slimmer technology will be incorporated into shirt sleeves as a wearable technology, further minimizing disruptions to patients who require repeated readings.

1.2 Objectives

To enable mechanistic testing of cuff size to blood pressure measurement, an anatomically and physiologically accurate arm simulator needs to be developed. Creating an arm simulator will allow for exact pressures to be set within the artery, which will be compared to the slim cuff reading to ensure accuracy. Several objectives were established to aid in the progression of the project:

- Perform a literature review to determine bicep dimensions and materials to simulate tissue, brachial artery, and bone for the construction of an arm simulator
- Design and fabricate an anatomically and physiologically accurate bicep for the purpose of testing the slimmer cuff
- Integrate alternating pressure system to simulate blood flow within the model artery

- Test alternating pressure system to ensure blood pressure measurements can be read using the industry-standard blood pressure cuff
- Design and construct a pressure sensor circuit for data acquisition

1.3 Design/System Requirements

To ensure precise and dependable blood pressure measurements in scientific and medical research contexts, we established a thorough set of system requirements for the anatomically and physiologically accurate model arm. The following table outlines the engineering requirements along with their justifications to meet these standards.

Engineering Requirements	**Reasoning**
The model arm must replicate the anatomical structure of the human arm to ensure realistic blood pressure measurements.	This requirement ensures that the arm's dimensions, tissue properties, and vascular structures closely match those of a human arm, enhancing the accuracy of the measurements.
The model arm should mimic physiological processes such as blood flow, arterial compliance, and pressure changes to simulate real-world conditions accurately.	Ensures that the arm behaves realistically during pressure measurements, providing reliable data for research purposes.
The materials used in constructing the model arm, including tubing and reservoir components, should closely match the mechanical and fluidic properties of human tissues and vessels.	Ensures minimal interference with pressure measurements and maintains physiological relevance in the experimental setup.
The fluid used in the reservoir should have specific properties, such as density and viscosity, to generate pressure changes detectable by the cuff.	Ensure adequate pressure changes, crucial for cuff detection, enhancing accuracy in simulating physiological conditions.

The system should measure blood pressure within the 95/90 confidence reliability interval of a cuff-based blood pressure measurement.	Ensures that the model arm's measurements are statistically reliable and comparable to standard cuff-based measurements, meeting the accuracy standards necessary for scientific and medical research.
The system must integrate pressure sensors capable of real-time monitoring and display of pressure measurements.	Enables direct and accurate measurement of blood pressure without relying on external commercial monitors.

Table 1: System Requirements

2.0 Background

There are many conditions that require frequent blood pressure measurements. Hypertension, defined as high blood pressure above 130/80, is one of the conditions that requires blood pressure monitoring for diagnostic and preventative treatment. The prevalence of hypertension within the United States is great; 119.9 million adults suffer from hypertension in the U.S. and 691,095 deaths in 2021 were a result of hypertension. The condition has a strong correlation with diabetes and puts patients at an increased risk for developing heart disease and stroke (Centers for Disease Control and Prevention, 2023). Thus, the need for monitoring hypertension through frequent blood pressure measurements is of paramount importance. Due to the large population of people with hypertension, the market for BP monitoring devices is growing at a rapid pace (Figure 1) (Grand View Research, n.d.). However, the primary means to monitor blood pressure measurements, the blood pressure cuff, has not undergone many advancements to enhance the patient experience and make the process quicker and more comfortable.

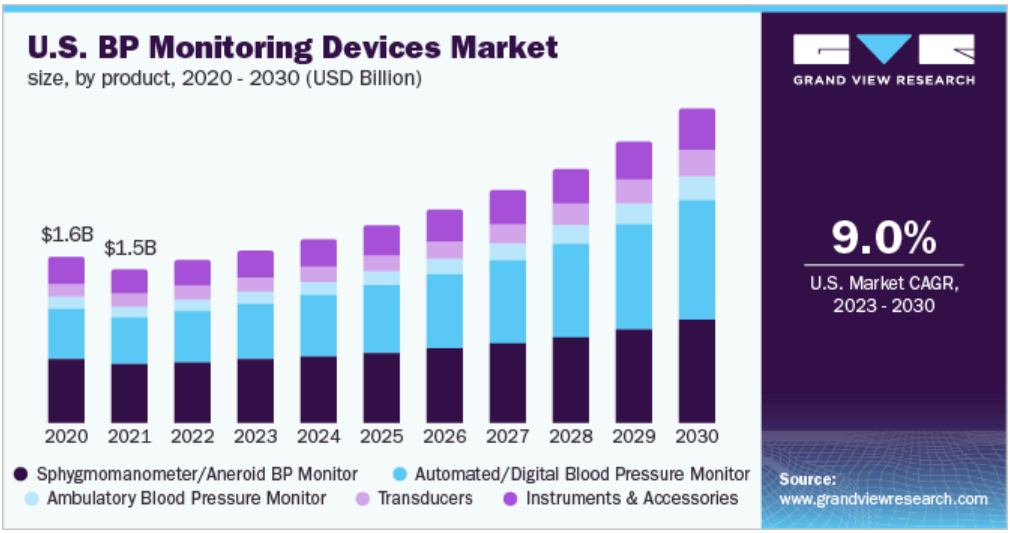

Figure 1: The demand for BP monitoring devices (Grand View Research, n.d.)

2.1 History of Blood Pressure Monitoring

The history of blood pressure monitoring dates back to 1733, when the first invasive blood pressure measurement was recorded. After William Harvey established that there is a finite amount of blood circulating within the body in the early 1600s, Reverend Stephen Hales recorded the first invasive blood pressure measurement conducted on a horse in 1733. His method involved inserting a brass pipe into the crural artery and securing a glass tube to the other end of the artery (Figure 2). The tube, positioned vertically, measured 8 feet 3 inches above the left ventricle of the horse's heart. Through this method, Hales measured the jugular venous pressure at rest and while excited, the left ventricle volume, output blood flow from the heart, and the blood vessels' resistance to flow (Roguin, 2005).

Figure 2: Reverend Hales records the first invasive blood pressure measurement (Roguin, 2005)

This technique would require refining before it would be feasible to measure a human's blood pressure. After further discoveries and advancements in the blood pressure field, Etienne-Jules Marey developed the Sphygmograph in 1860, enabling the graphical recording of blood pressure variations and pulse features. Further advancements were made to Marey's Sphygmograph to make the device portable. Robert Ellis Dudgeon improved upon Marye's Sphygmograph to make it portable by strapping the device to the wrist. The wrist's pulse triggered the movement of a stylus that recorded the pulse on paper, recording blood pressure and pulse continuously over time (Figure 3) (Roguin, 2005)

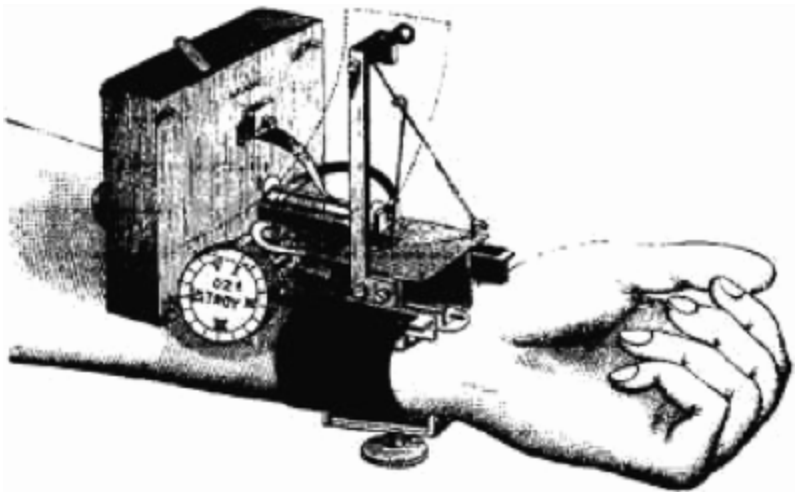

Figure 3: Robert Ellis Dudgeon's portable blood pressure device (Roguin, 2005)

Up until the 1880s, the methods for recording blood pressure required inserting a tube into an artery. In 1881, Samuel Sigfried Karl Ritter von Basch overcame this limitation in blood pressure technology by developing a technique to gather blood pressure measurements non-invasively using a mercury column. Unfortunately, his method proved inefficient and was not adopted widely in the field. However, building off of the advancements in the blood pressure monitoring field, Scipione Riva-Rocci successfully developed a mercury sphygmomanometer in 1896; this invention would spark the invention of the modern-day blood pressure cuff technology by Hill and Berard in 1897. Their apparatus consisted of an inflatable cuff that encircled the forearm (Science Museum Group, n.d.). Using a needle pressure gauge, the cuff tightened around the arm, and as pressure within the cuff slowly released, systolic pressure oscillations were recorded. Diastolic pressure oscillations were measured by taking the difference between the maximum oscillations and the smaller oscillations (Roguin, 2005). Changes to cuff dimensions were made over the next few years to achieve today's modern cuff.

2.2 Technology Behind Today's Blood Pressure Cuff

In clinical settings, various technologies are employed to accurately measure blood pressure, each offering distinct advantages and limitations. These technologies cater to different patient needs and clinical scenarios, ensuring precise and reliable blood pressure readings. The

following table (Table 1) outlines some of the current methods used in clinical practice, highlighting their respective strengths and constraints.

	Method of measurement	Advantages	Limitations
Korotkoff	A manual auscultatory technique where the cuff is inflated and slowly deflated while the practitioner listens over the brachial artery for Korotkoff sounds (phase I–V)	Clinical "gold standard" for non-invasive monitoring Inexpensive No risk to patient	Relies on "trained" personnel. Subjective method with possible human error. Cuff sizing errors Cannot be done continuously
Oscillometric	An automated technique where the cuff is inflated and slowly deflated while a pressure sensor detects oscillations	Convenient Inexpensive Requires little to no operator skill	Cuff sizing errors Cannot be done continuously
Arterial line	Direct arterial catheterization (radial, femoral, brachial, etc.) connected through a fluid column to a pressure transducer	"Gold standard" for invasive monitoring Continuous monitoring	Risk to the patient Requires "trained" personnel to place appropriately
Peñás	Volume clamp method which utilizes a finger cuff that adjusts pressure order to keep optically measured finger vascular volume constant	Convenient Non-invasive Continuous monitoring	Expensive Affected by factors such as cold extremities, vasopressors Needs calibration via another method.

Tonometry	Uses applanation (flattening) of the radial artery and measures pressure transmitted through the skin	Non-invasive Continuous monitoring	Expensive Manual positioning of tonometer over radial artery not always accurate
Pulse transit time (photometric)	Pulse transducers located at two different sites record the time it takes for an arterial wave to travel between these two points	Non-invasive Continuous monitoring Requires no additional monitors over standard ASA monitors	Not fully developed to correlate pulse transit time to blood pressure

Table 2: Commonly used techniques for blood pressure monitoring (Chung et al, 2013)

The most commonly used technique for measuring blood pressure is intermittent automated oscillometric measurement. This method involves using an inflatable, occluding cuff placed on the upper arm, which is then gradually deflated while monitoring the pressure inside the cuff. Typically, this method measures blood pressure over intervals of 3 to 5 minutes. The accuracy of this measurement technique depends on the size of the cuff relative to the circumference of the upper arm, which is why there are different cuff sizes available for different individuals. Using the correct cuff size ensures that the pressure applied to the artery is measured accurately, as an improperly sized cuff can lead to inaccurate readings (Saugel & Sessler, 2021).

When the oscillatory cuff is inflated, it temporarily stops blood flow through the artery. As the cuff is deflated below the systolic pressure, allowing blood to flow, a detectable vibration occurs in the arterial wall. This vibration is caused by the blood pressure being high enough to push the arterial wall open to allow blood flow. The cuff pressure falling below the patient's diastolic pressure allows blood to flow smoothly through the artery without causing vibrations on the arterial wall, as in a normal pulse rate. These vibrations are then transmitted from the arterial

wall through the air inside the cuff to a transducer in the monitoring device. Figure 4 below depicts this process.

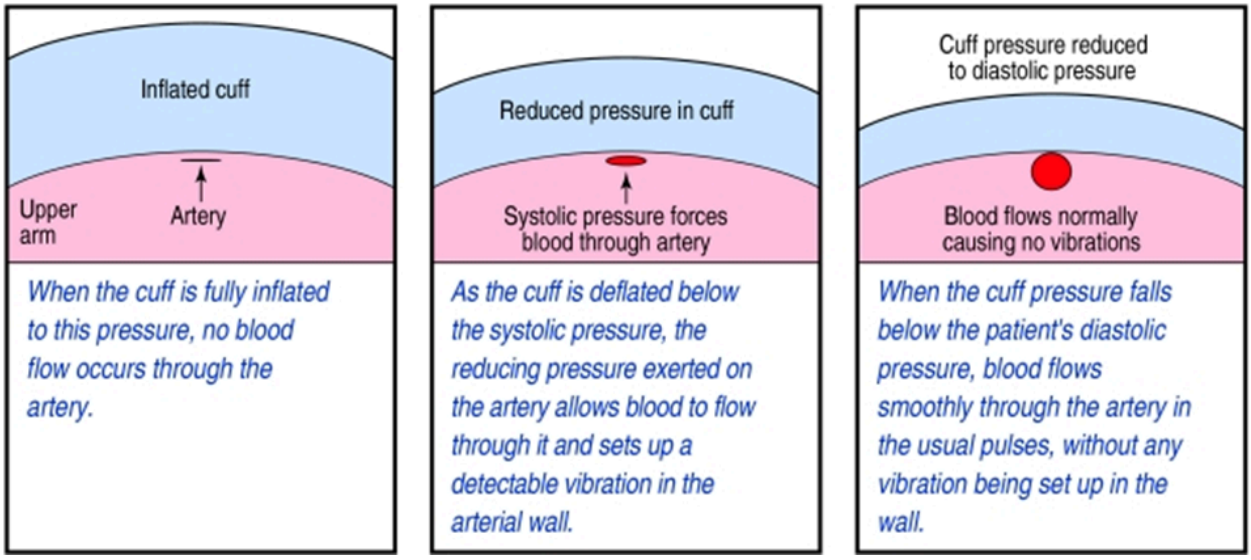

Figure 4: Oscillometric blood pressure cuff at different inflation levels (Berger, 2001)

The transducer converts these vibrations into electrical signals, which are then used to determine and display the blood pressure readings. The monitoring device processes these electrical signals using algorithms to calculate the systolic and diastolic blood pressure values. This information is displayed on the monitor screen and may also be recorded for further analysis or to create a blood pressure history for the patient (Berger, 2001).

3.0 Methods

To satisfy the objectives in Section 1.2, several methods were followed. First, a literature review was performed to determine the materials and dimensions for constructing an arm simulator. Using the findings from the literature review, an arm simulator was modeled and fabricated. Then, an alternating pressure system and data acquisition system were incorporated.

3.1 Material Selection

A literature review was performed to determine material selection for the creation of a model arm. Sparks, et al. examined three silicone materials that have shear moduli values within the range of biological tissue (Figure 5). In their research, the shear modulus for Ecoflex 0030

silicone fell within the upper range of biological tissue and was used to simulate skin. The Dragon Skin silicone displayed compressive properties representative of active muscle and was used to simulate muscle. Finally, Ecoflex 0010 silicone had the lowest shear modulus and was used to simulate fat (Sparks et al., 2015).

Table 2.

BEST-FIT HYPERELASTIC MATERIAL CONSTANTS FOR SILICONE RUBBER FORMULATIONS

	Ogden Model Terms		
Silicone Type	Shear Modulus G (kPa)	Strain Hardening Exponent α	Poisson Ratio ν
Dragon Skin	75.449	5.836	0.4999
Ecoflex 0010	12.605	4.32	0.4999
Ecoflex 0030	22.081	0.825	0.4999

Figure 5: Material properties of silicone varieties that represent biological tissue (Sparks et al., 2015)

Additionally, research into the properties of the brachial artery was conducted. The average Young's Modulus of the brachial artery is 3.8±1.7 MPa (Leguy et al., 2010). The best commercially available material that resembles the modulus of the brachial artery was found to be rubber, with a Young's Modulus of 3 MPa, falling within the average Young's Modulus for the brachial artery (*Natural Rubber*, n.d.).

3.2 Model Arm Design

To manufacture an anatomically accurate arm, it was essential to research the average dimensions of the humerus and the brachial artery, and their relative positions to one another and to the skin. This information would be used to model and 3D print a mold in which to cast the silicone arm. The relevant dimensions and sizes used were based on those given by Lan et al. in Figure 6 below (Lan et al., 2011).

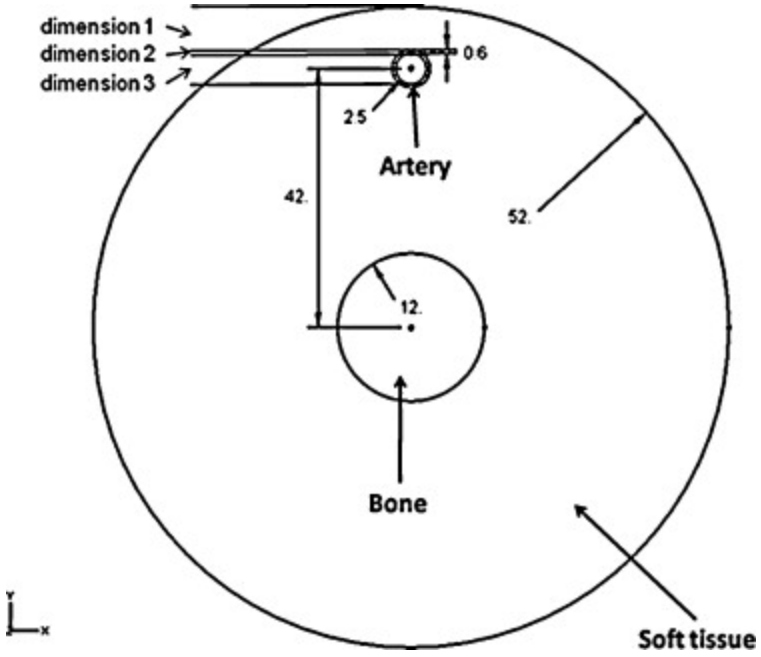

Figure 6: Cross section of upper arm depicting position and size of brachial artery and humerus (Lan et al., 2011)

The size of the humerus and the brachial artery were constrained by the available off-the-shelf PVC pipe and rubber tube dimensions, respectively. Therefore, a PVC pipe and rubber tube with dimensions closest to those depicted in Figure 6 were chosen. A PVC pipe with an outer diameter of 21.4 mm was found on amazon to best represent the humerus diameter, and a rubber tube with an inner diameter of 3 mm and a wall thickness of 1 mm was found on amazon to best represent those corresponding dimensions of the brachial artery depicted in Figure 6. The artery was modeled parallel to the humerus along its entire length without any bends for ease of manufacturing. The average maximum length of the humerus was found to be 304.56 +/- 14.16 mm (Khan et al., 2020). However, the length was also constrained by the PVC pipe. A humerus length, and therefore arm and artery length, were chosen to be 280 mm, a length that falls close to the researched range. These dimensions were used to design a mold to cast the silicone in. Once the silicone cured around the PVC pipe and rubber tube, the mold was removed, leaving behind a successfully modeled arm. The assembled mold with the PVC pipe and rubber tube is depicted in Figure 7 below.

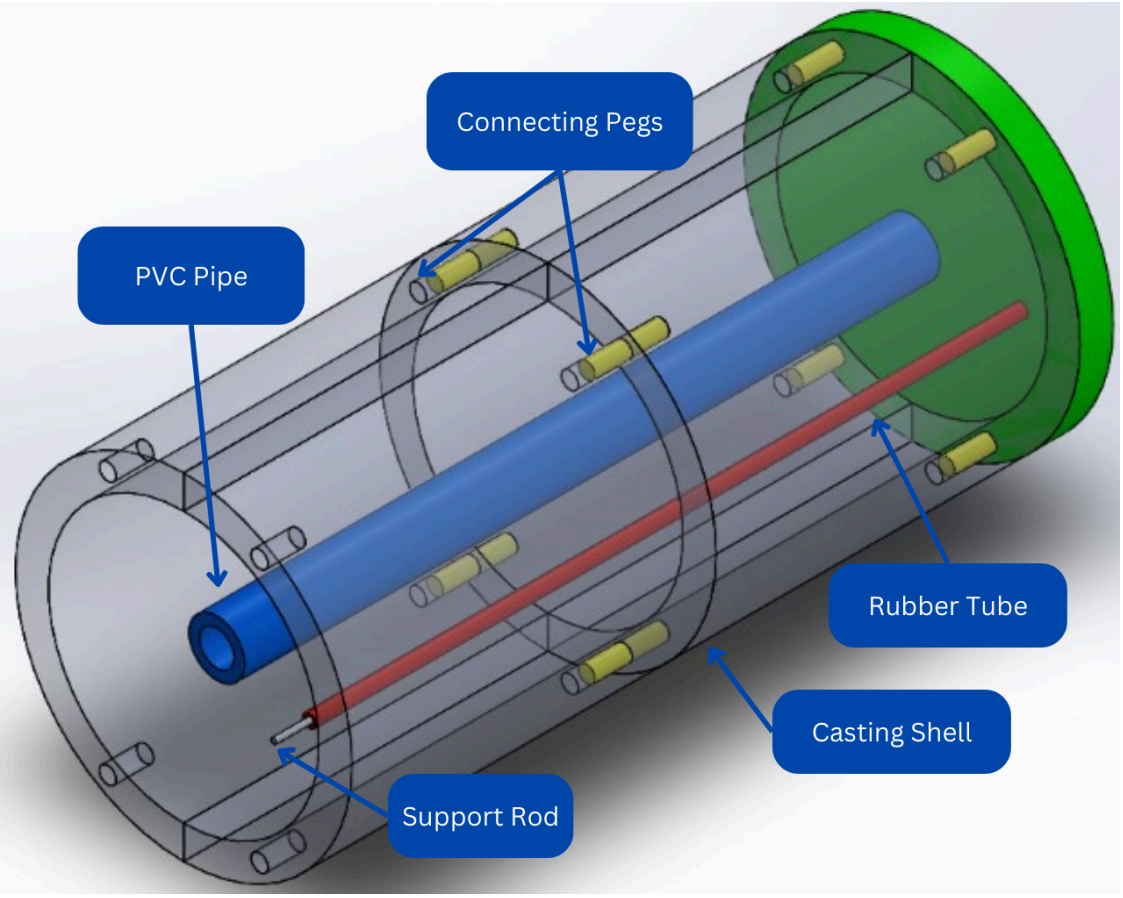

Figure 7: CAD model of silicone mold

The assembly model of the designed silicone mold created in SolidWorks is displayed above in Figure 7. The semi-circles (transparent) that make up the body of the cast are attached to one another and to the base (green) with the wooden dowels (yellow). The base and semi-circles were 3D printed and the wooden dowels (yellow), PVC pipe (blue), rubber tube (red), and metal support rod for the artery (gray) were purchased from Amazon. The dimensioned drawings of the 3D printed parts can be found in Appendix A.

3.3 Casting Procedure

After conducting the literature review to gather proper dimensions and materials for modeling the upper arm, we began prototyping. In an effort to simplify the model, one silicone type was used to simulate the skin, muscle, and fat within the arm, a PVC pipe represented the humerus, and a rubber tube represented the brachial artery. First, we 3D printed and assembled

the mold for the arm. The mold, shown earlier in Figure 7, consisted of 4 panels, a base, and a lid. These components were connected by wooden dowels. In this manner, the mold was printed in sections that fit the sizing constraints of the available 3D printers. Additionally, separate panels allowed for easier removal of the silicone model arm once cured. We assembled the mold with the 4 side panels, attached them to the base with wooden dowels, and prepared the mold with a release agent. Leaving the top open, we inserted the PVC pipe and rubber tube into the respective holes in the base. A metal rod was inserted into the artery to support the tube throughout the curing process. Next, the silicone was mixed according to the manufacturers' instructions. Then, we poured the silicone into the mold, focusing on pouring down the inner side of the mold to minimize the introduction of air bubbles into the silicone. Once filled, we placed the cap onto the mold, inserting the top of the pvc pipe and artery into their respective holes in the cap. This ensured that the PVC pipe and artery were straight and in the proper place while the silicone cured. After the allotted curing time, we removed the mold from the silicone to reveal the model arm.

3.4 Testing Silicone Types

Initially, we tested the arm model using Dragon Skin silicone and used baby powder as the release agent from the mold (Figure 8). The release agent worked well because the Dragon Skin silicone does not have a tacky finish. However, because the Dragon Skin silicone represented active muscle, the resulting model arm was too hard and was unable to be manually deformed to partially collapse the artery. Thus, we deduced that the blood pressure cuff would not be able to generate a reading using this model.

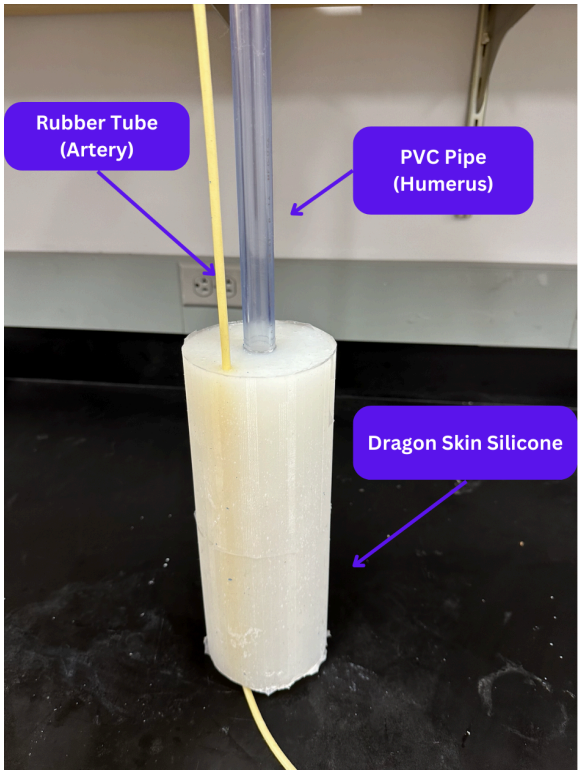

Figure 8: Model arm casted using Dragon Skin silicone

We shifted to use Ecoflex 0010, representing fat, as the material for the model arm. Initially, we used baby powder for the release agent from the mold. Unfortunately, since Ecoflex 0010 has a tacky finish when fully cured, the baby powder did not work well as a release agent, and we were unable to remove the cured silicone from the mold. It took many attempts to remove one panel since the silicone was stuck to the plastic. After successfully removing one panel of the mold, the silicone underneath was torn resulting from the tools used to pry the silicone from the mold (Figure 9).

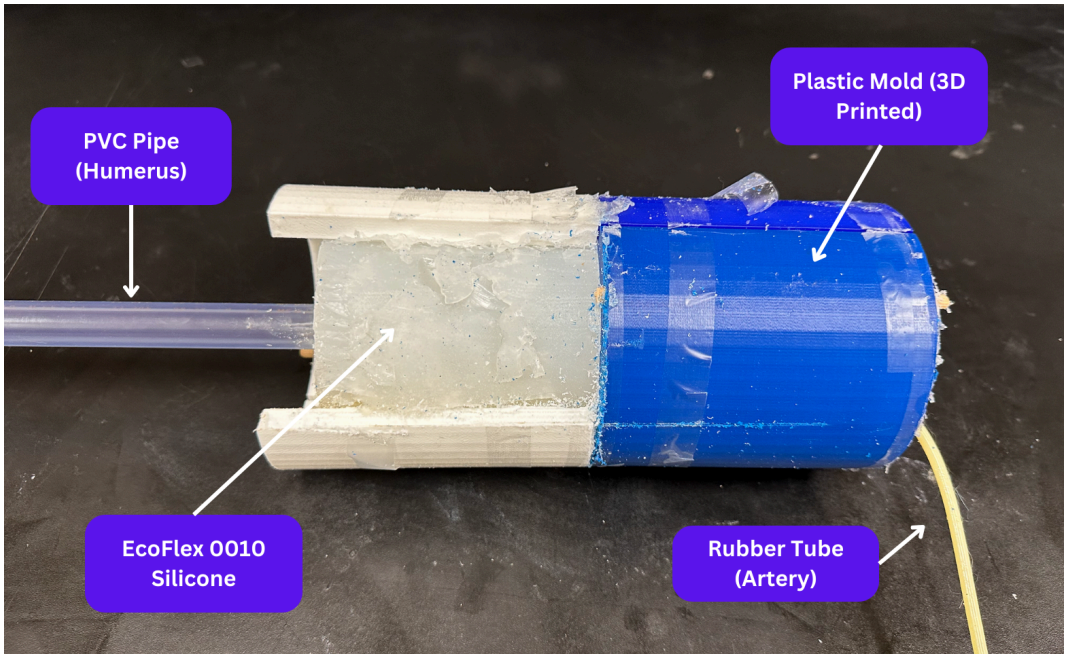

Figure 9: Baby powder was not an effective release agent for Ecoflex 0010 silicone

We printed a new mold and used Ease Release 200 as the release agent. Using this, we were able to successfully remove the cured silicone from the mold (Figure 10). We found that this material could be manually deformed easily, allowing for the artery to be partially collapsed. This was the arm model we used throughout the subsequent experiments.

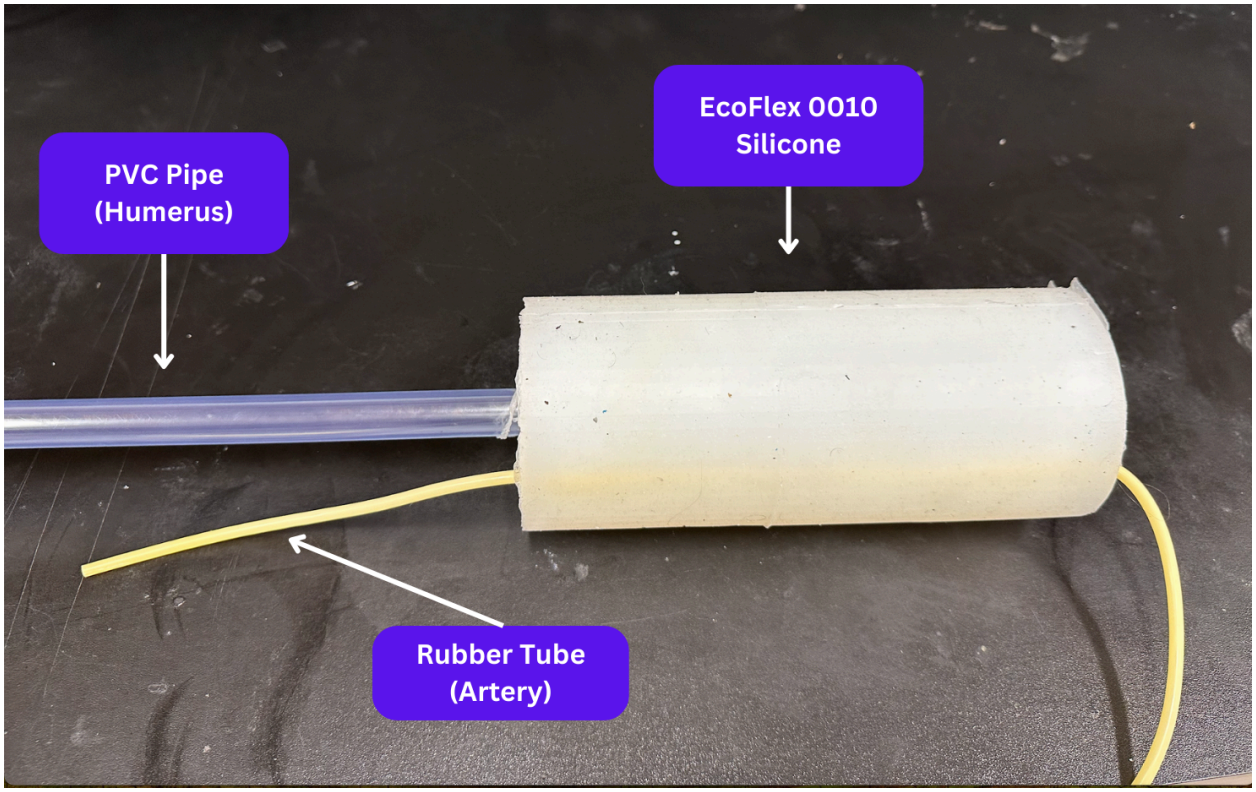

Figure 10: Ecoflex 0010 silicone arm model used throughout subsequent experiments

3.5 Experimental Setup

To prove the feasibility of the model arm, we tested whether the blood pressure monitor would be able to detect a blood pressure with pressure changes in the artery. The experimental setup consisted of attaching the artery to a water reservoir at atmospheric pressure, filling the artery with water, and tying off the end of the artery where the water exited the arm model. We placed the arm model on the ground with the blood pressure cuff wrapped around the arm and moved the water reservoir from 1m to 1.5m above the arm to produce a 40mmHg (average pulse pressure) pressure change (Figure 11 and 12) (Homan, 2023). The change in height of a reservoir of static fluid is related to its pressure change according to the following equation:

$$\Delta P = \rho * g * \Delta h \quad (1)$$

Where ΔP represents the change in pressure, ρ is the density of the fluid, g is the acceleration due to gravity, and Δh is the change in height. Rearranging equation (1) for the change in height, setting the change in pressure to the average pulse pressure, and plugging in the

density of water gives a change in height of 0.5 meters. The initial height of 1m corresponds to a pressure of 70mmHg. We manually moved the reservoir this distance with a frequency of 1 Hz while the blood pressure cuff inflated and deflated. Theoretically, the pressure change between the two distances should have generated a large enough pressure difference for the blood pressure monitor to produce a reading. However, with each test we ran using this method, we were unable to get a pressure reading, and the blood pressure monitor gave us an error.

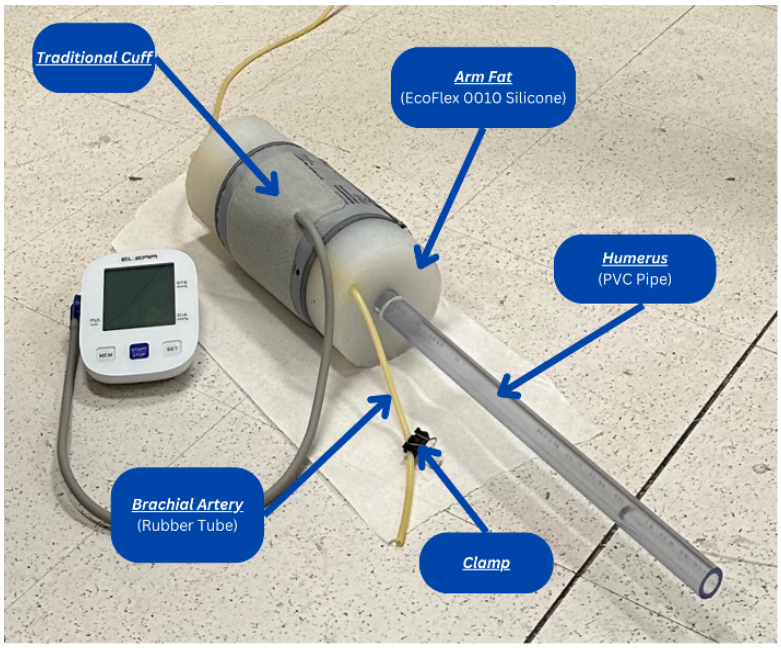

Figure 11: Model arm connected to the industry-standard blood pressure cuff

Figure 12: Experimental setup for changing the pressure by manually moving the water reservoir

3.6 Generated Hypotheses

From the inconclusive results of this initial testing, we generated three hypotheses regarding why the experimental method was not producing a blood pressure reading:

- Hypothesis 1: Variability in the water reservoir height and speed attributed to human error simulates an erratic and unrealistic heartbeat that the monitor is unable to produce an accurate reading from. While manually moving the reservoir from 1m to 1.5m at 1-second intervals, there were inconsistencies in the height and the pacing throughout each cycle.
- Hypothesis 2: The blood pressure monitor might be measuring a pressure variation, but it reports an error message because it may be too small of a change to produce an accurate diagnosis.

- Hypothesis 3: The water being used to represent blood through the artery does not have a high enough density to produce a sufficiently large pressure change.

3.6.1 Testing Hypothesis 1

To test the validity of the first hypothesis, the water reservoir's motion was automated through the use of an Arduino Uno controlled Nema 23 stepper motor. The circuit to automate this motion is depicted in Figure 13 below.

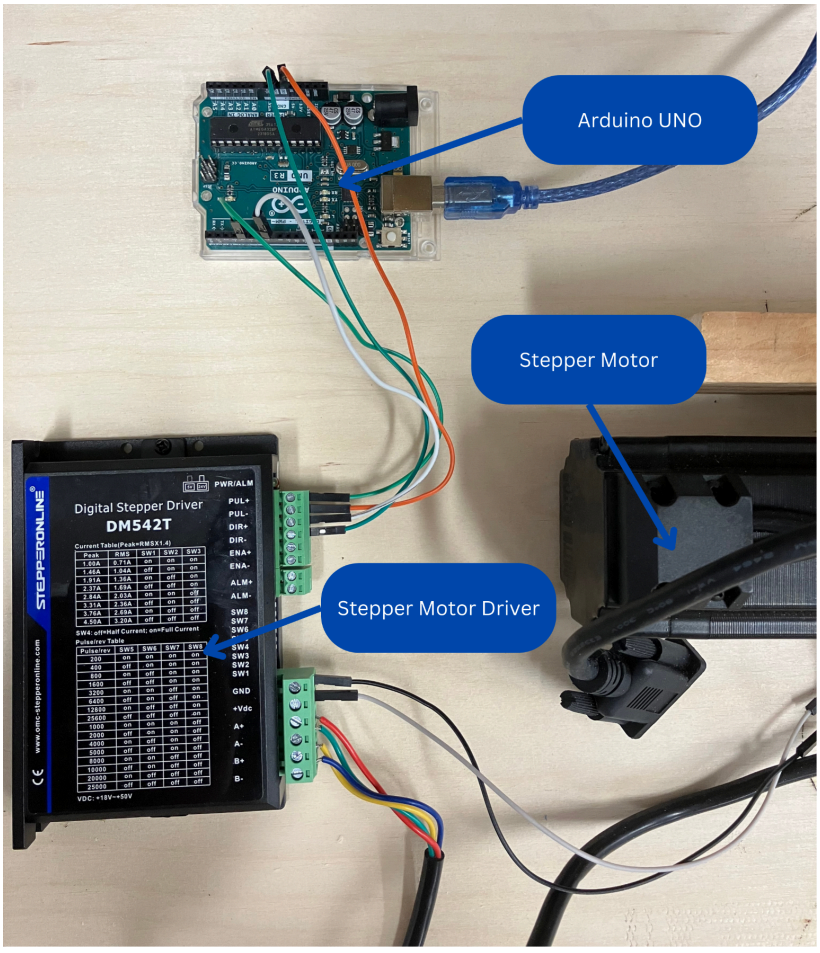

Figure 13: Arduino Uno controlled stepper motor circuit

The circuit in Figure 13 above connects the digital stepper driver with the Arduino Uno and Nema 23 stepper motor powered by an external DC power supply. The PUL+ and DIR+

terminals on the stepper driver are connected to the analog pins 4 and 7 on the Arduino Uno, respectively. The PUL- and DIR- terminals are grounded to the Arduino. The ground and +Vdc terminals on the driver are connected to ground and power on a DC power supply. The red, green, yellow, and blue wires from the stepper motor are connected to the A+, A-, B+, and B- driver terminals, respectively. The driver settings are set to be: 5V, 2.37A, full current, and 200 Pulse/rev. The power supply provides 24V to the system.

By automating the height change and speed, human error was eliminated to allow for a consistent pressure change every cycle. The stepper motor was programmed to travel at a certain speed with a certain acceleration and then change direction once it steps a certain number of times. From our testing, we determined that 1,352 steps from the motor corresponds to a distance of half a meter along the linear actuator. Therefore, the reservoir was automatically moved from 1m above the arm to 1.5m and then back again in about 1.2 seconds. This was the fastest the motor could be programmed without disrupting the actuator's smooth motion. The full Arduino IDE code can be found in Appendix B. A frequency of 1 Hz was desired to simulate a heartbeat of 60 beats per minute, but as mentioned, the stepper motor's speed was capped by the physics of the linear actuator. Instead, the automated setup simulated a heartbeat of 50 beats per minute. This is still a reasonable heartbeat for a healthy individual. The reservoir started at 1m above the arm and moved to 1.5m to simulate a diastolic and systolic blood pressure of about 73 mmHg and 110 mmHg, respectively given by equation (1). These numbers also fall within the healthy range of blood pressure values. The difference between the systolic and diastolic values therefore, known as the pulse pressure, is 37 mmHg, which is close to the average value of 40 mmHg (Homan, 2023). Overall, the automated setup simulates a consistent and accurate cardiac cycle for a healthy individual. Figure 14 below depicts the full automated setup.

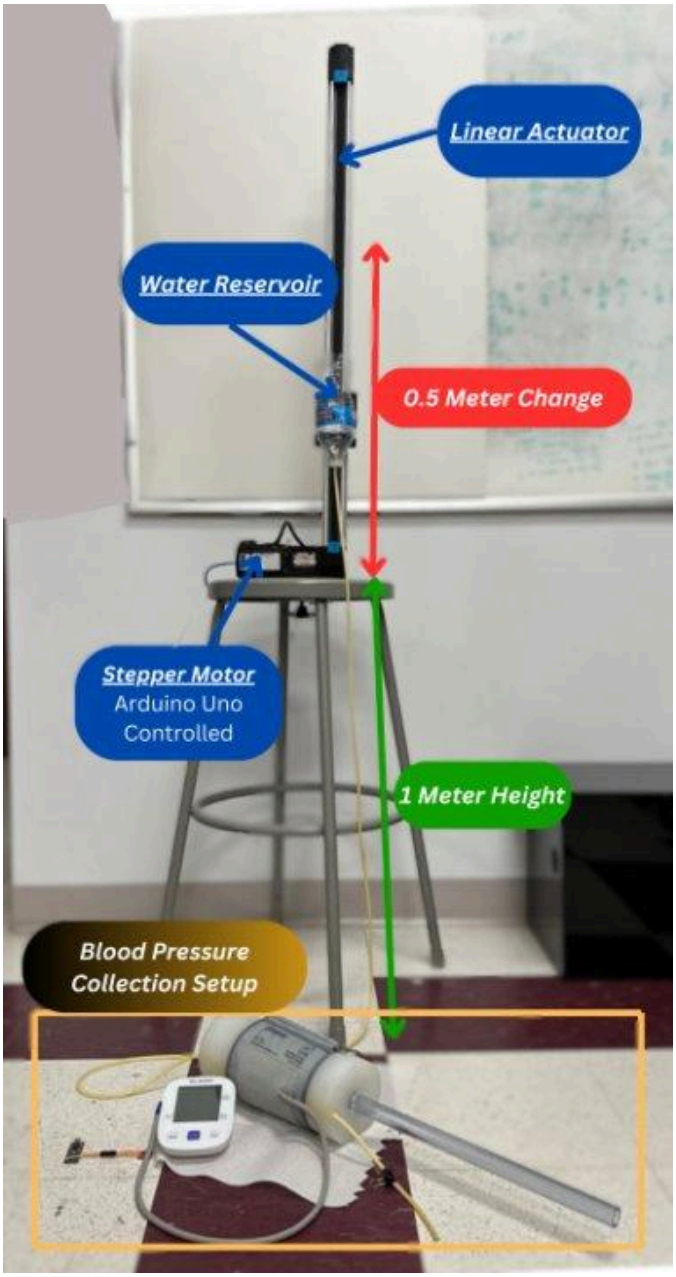

Figure 14: Automated alternating pressure system

After testing this new setup, it was found that the blood pressure monitor could still not provide an accurate reading; it would produce the same error message as before when moving the reservoir manually. Automating the motion made the testing process more efficient and more consistent, but it did not solve the problem of generating an accurate reading for the monitor to display. Upon touching the rubber tube, a consistent pulse could be felt in time with the water

reservoir's vertical displacement, but this same pulse could not be felt through the silicone. It was possible that either the silicone was dampening the pressure change such that the monitor was reading too little of a value to display, or it was blocking the cuff from reading any pressure change at all. It became essential, therefore, to display and analyze the real time pressure readings from the cuff as it inflated and deflated around the model arm. Doing so will test the second hypothesis generated: whether the cuff is reading a pressure change and what that pressure change looks like.

3.6.2 Testing Hypothesis 2

To test Hypothesis 2, we needed to determine if we could use the sensor within the blood pressure monitor to collect data by attaching an arduino nano directly to the pressure sensors within the monitor. To do this, we needed to locate the sensor within the OMRON M3 Digital Blood Pressure Monitor and take readings directly from the sensor before they are processed by the OMRON M3 program. We soldered two wires to the pressure sensor pins to be read by the arduino Nano (Figure 15).

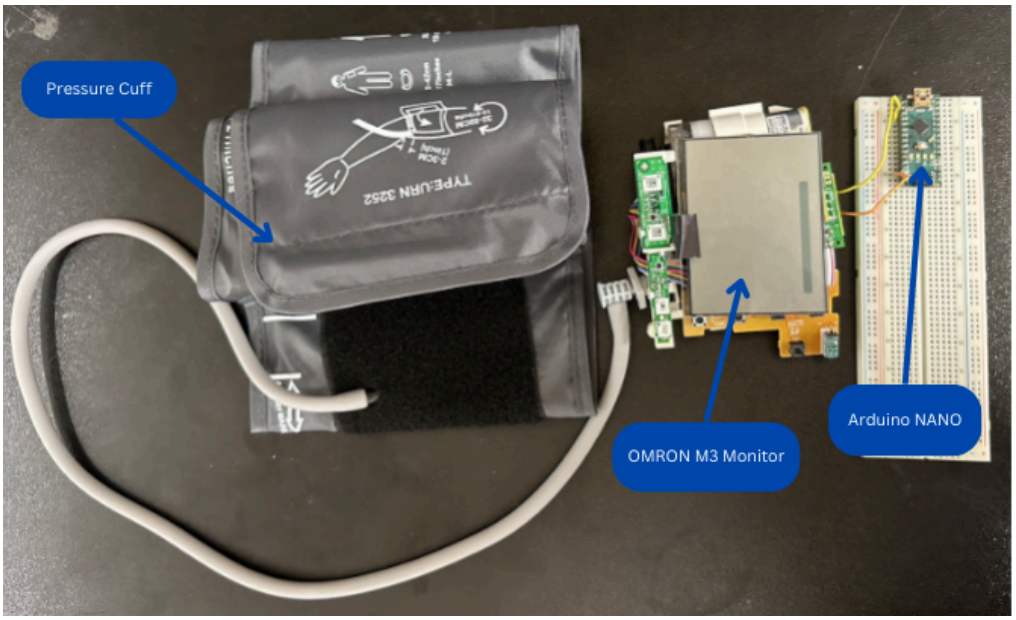

Figure 15: Arduino Nano direct connection with OMRON M3 Digital Blood Pressure Monitor

However, the readings we received by connecting the Arduino Nano directly to the pressure sensors within the OMRON M3 Digital Blood Pressure Monitor were only able to

produce a square wave showing 1's and 0's (Figure 16). These square waves were not helpful to show a change in pressure that is used to produce blood pressure measurements.

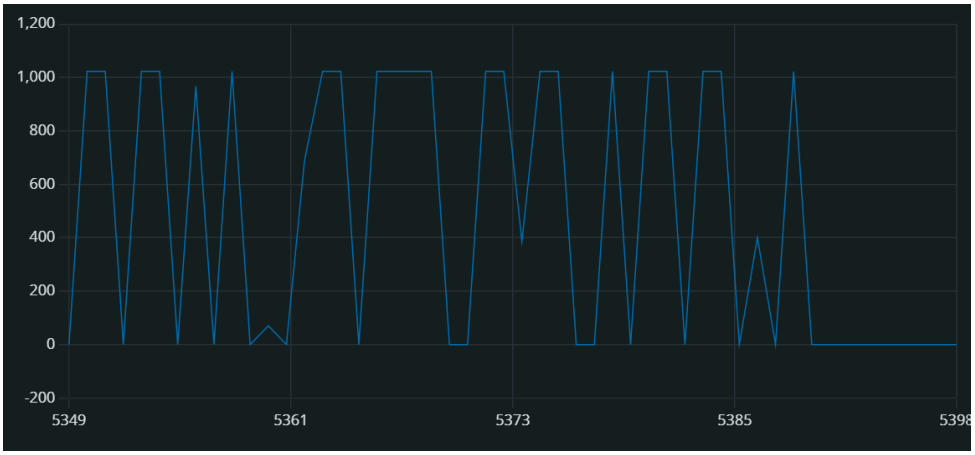

Figure 16: The square wave produced from the OMRON M3 pressure sensors

The readings we were gathering were actually an incomplete signal. Dr. Zhang at Massachusetts General Hospital (MGH) informed us that these types of pressure sensors in commercial use have a three pin configuration instead of the assumed two pin for signal amplification. Because we weren't able to obtain a schematic of the system to find the third pin due to copyright we shifted toward previewing circuit designs using a plastic circuit board (PCB) that MGH used previously for their testing of the slim cuff.

3.7 Data Collection

The recording of data was carried out through the modification of a digital blood pressure monitor. To modify the monitor to allow us to take direct pressure measurements from the system, we used an Arduino Nano connected to a PCB containing an MSP40-GSF pressure sensor and TM7711 chip. The pressure sensor was inserted directly into the tube connected to the pressure cuff (Figure 17). By connecting the pressure sensor this way, we were still able to use the automated pump within the digital blood pressure monitor to inflate and deflate the pressure cuff.

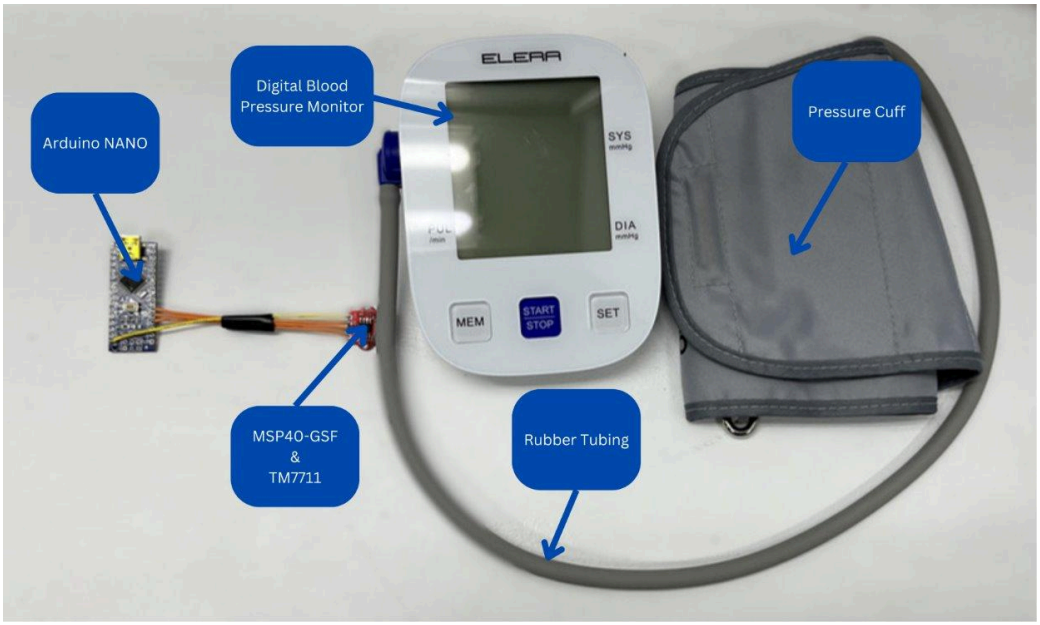

Figure 17: Final data acquisition setup

The setup and calculation code developed by previous teams was provided by MGH. The code was broken up into two parts. The first was an Arduino code that set up the pin configuration for the Arduino Nano to communicate and read pressure readings (Appendix C). The second was a MATLAB code that was used to collect the data from the cable port (Appendix D). The MATLAB code also includes the calculations for pressure measurements such as systolic, diastolic blood pressure, heart rate, and mean arterial pressure along with visual plots (Appendix D).

4.0 Results

With the final data acquisition setup and code completed, we were able to conduct testing. The tests consisted of using both a human arm and the model arm to collect the raw pressure readings throughout the cuff's inflation and deflation over time. These results are illustrated in Figures 18 and 19 below.

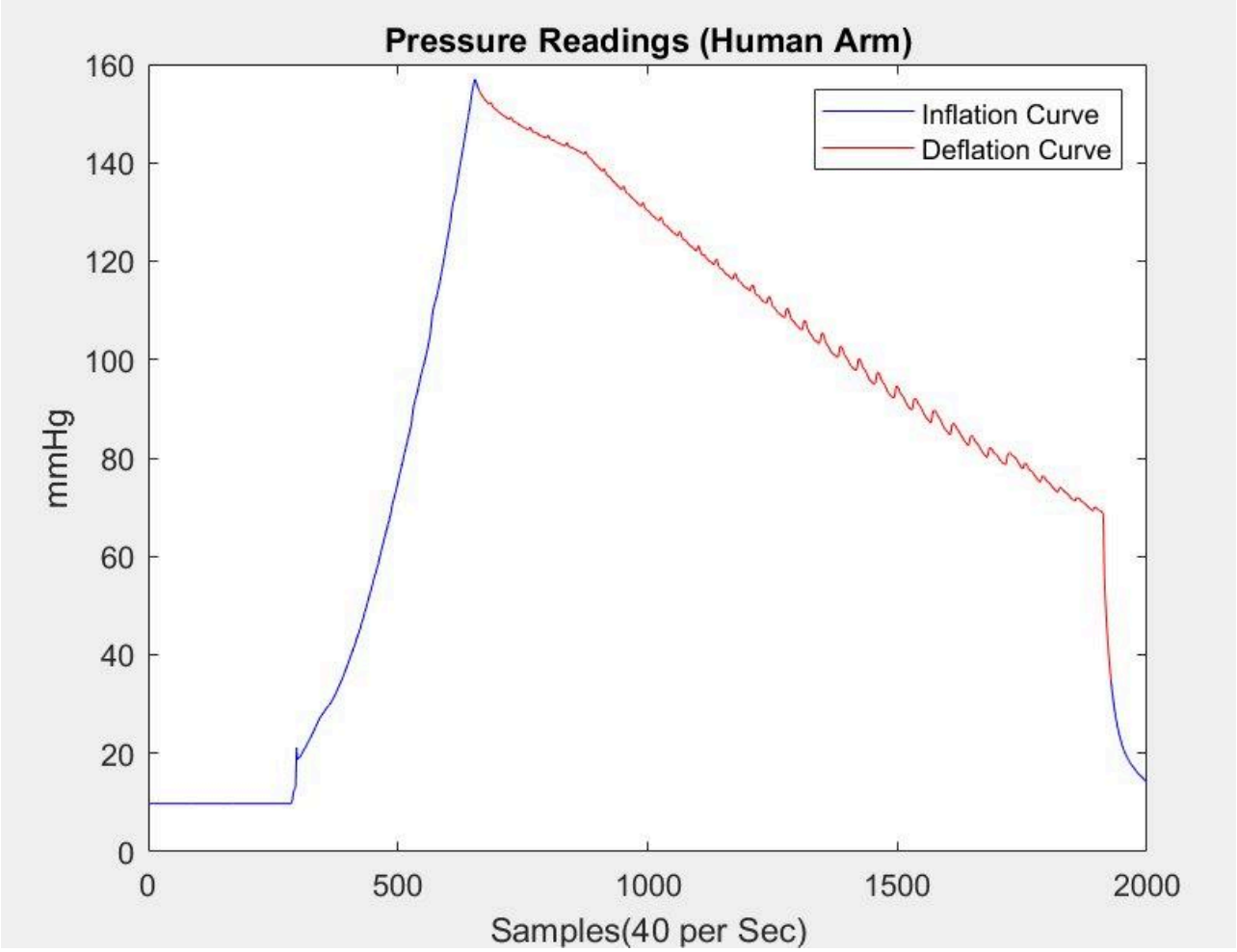

Figure 18: Inflation and deflation curve of cuff pressure on human arm

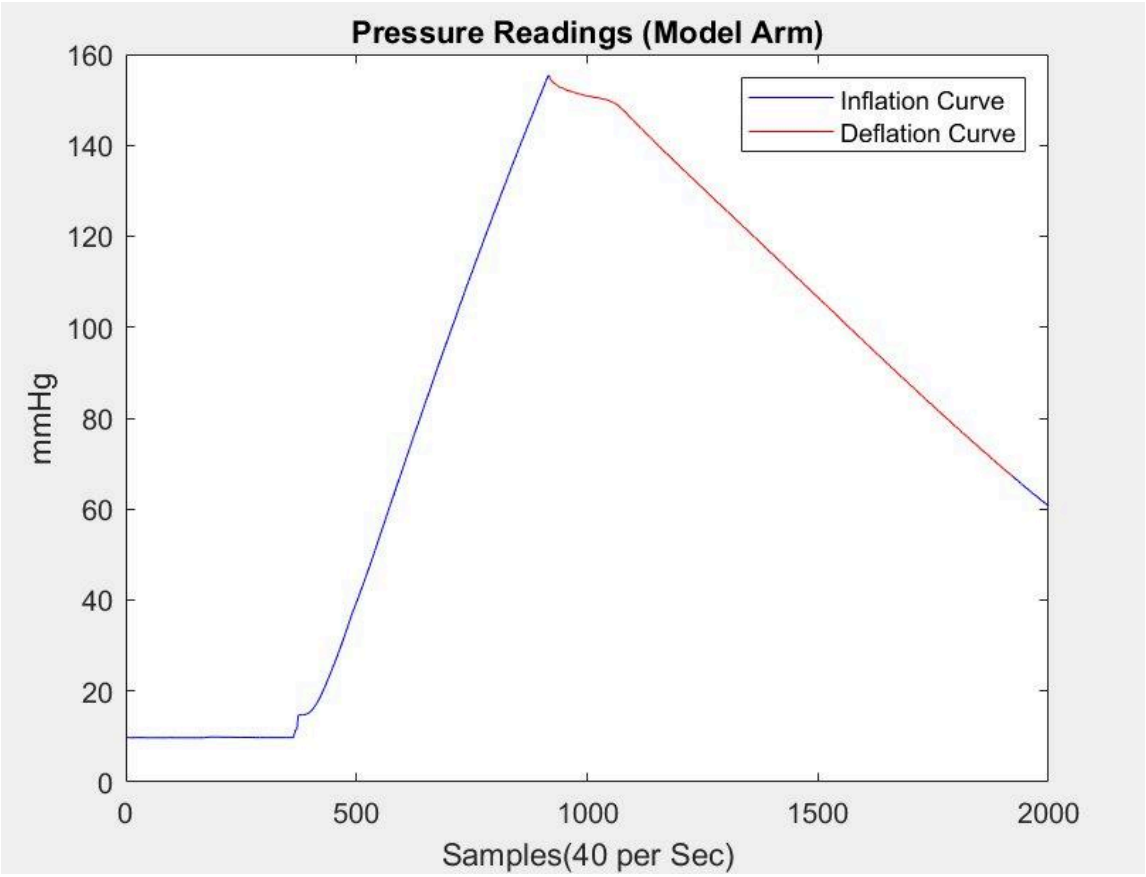

Figure 19: Inflation and deflation curve of cuff pressure on model arm

As the blood pressure cuff inflates around the human arm in Figure 18, the pressure does not increase linearly like it does as it inflates around the model arm in Figure 19. This is because a human arm is viscoelastic whereas the model arm is made out of silicone, an elastic material. As the cuff deflates around the arm, the blood pressure monitor records the pressure difference between the cuff's set pressure and the pressure the cuff feels from the arm. This data is used to calculate the mean arterial blood pressure (MAP) which can then be used to back calculate the systolic and diastolic blood pressures. The measured differences in pressure during deflation can be seen in the human arm, but not in the model arm. To understand why and exactly what was happening during this region, the MATLAB code plotted this data zoomed in on new graphs. The zoomed in pressure differences recorded during the cuff's deflation around the human and model arm are depicted below in Figures 20 and 21.

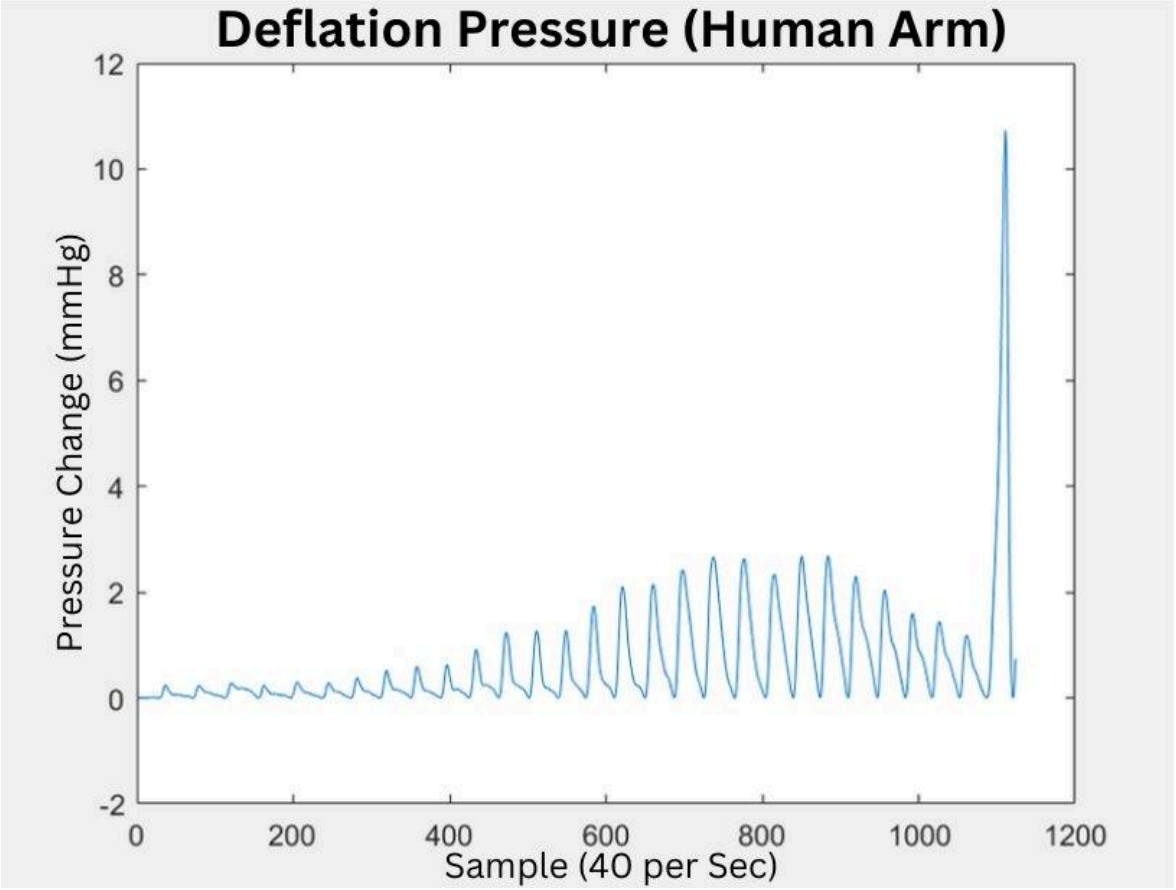

Figure 20: Human arm pressure difference during deflation

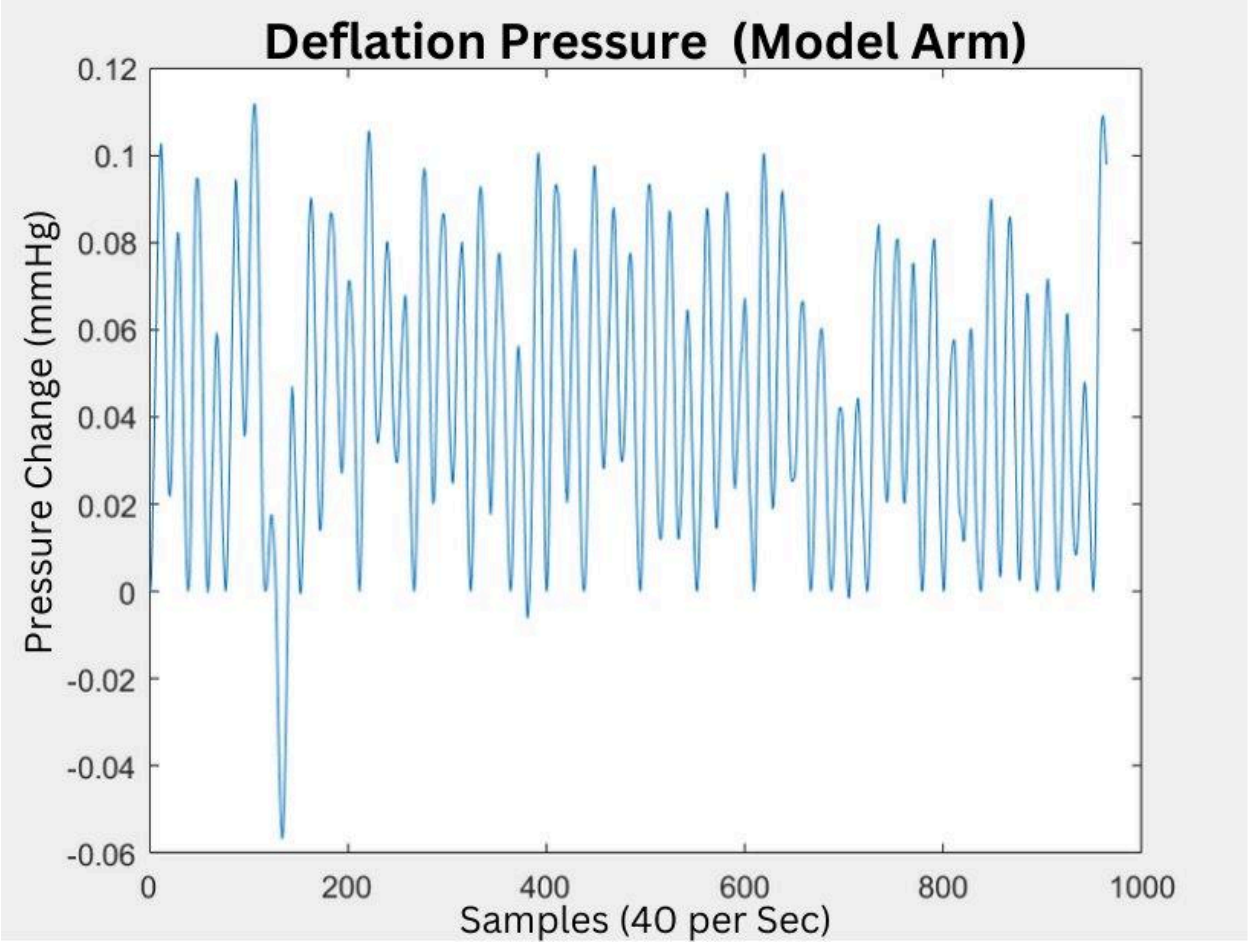

Figure 21: Model arm pressure difference during deflation

Figure 20 illustrates a present heartbeat. Initially no pressure difference is measured between the cuff and the arm because the cuff's pressure is greater than the systolic blood pressure. As the cuff continues to deflate to lower pressures, it begins to feel the blood pressure in the arm. Eventually it reaches a maximum value and then drops back to 0 mmHg when the cuff deflates to a pressure less than the diastolic blood pressure. The end behavior of Figures 18 and 20 represent the same phenomenon: the rapid deflation of the blood pressure cuff after it has deflated past diastolic pressure, indicative of its success in measuring an accurate blood pressure.

However, this end behavior is not seen in Figures 19 and 21. The cuff continues to deflate in Figure 19 until the monitor provides an error message; it appears that no differences in pressure were detected by the cuff between its pressure and the model arm's pressure as it slowly deflated around it. In other words, it appears that the blood pressure cuff could not measure a

simulated heartbeat in the model arm; it could not feel the pressure change of the water in the rubber tube. Figure 21 provides more information and displays a pressure difference on the order of two magnitudes smaller to that in Figure 20. Compared to the human arm, the reading from the model arm does not change over time. There are two possible explanations. The first, is that this data could be noise, and in fact the blood pressure cuff is not reading a pressure from the model arm at all. The second, is that the cuff is reading a pressure, but it is so small that the monitor does not believe it to be from a heartbeat and displays an error instead of extracting a physiologically inaccurate MAP. These two theories require more future testing to explore.

5.0 Discussion and Recommendations

Our project has achieved significant milestones in developing an anatomically and physiologically accurate model arm for efficient testing. Realistic anatomical features, including the brachial artery and surrounding tissues, were incorporated, resulting in an arm that closely resembles a human limb. Future enhancements could involve adding additional tissues such as capillaries and veins to improve the accuracy of blood pressure readings. Redesigning the model arm with arterial branching, where tubes branch in various directions to mimic the brachial artery's structure, can significantly enhance cuff detection of pressure changes. This modification has the potential to amplify the system's sensitivity, resulting in more precise and reliable blood pressure readings and laying a strong foundation for future research, particularly in evaluating the impact of cuff sizes on blood pressure measurements.

Additionally, our project introduced a mechanism for automatically adjusting the height of a static fluid reservoir, thereby modulating the fluid pressure within the model arm. This innovation effectively controlled pressure levels during testing, demonstrating its potential for precise pressure management. However, there are opportunities for enhancing the setup's aesthetics and functionality. Suggestions include replacing the current reservoir—a half-cut water bottle attached with glue—with a more refined alternative. Organizing and securing the Arduino Uno, Stepper Driver, motor, and actuator onto a main baseboard can also improve the setup's organization and durability, ensuring consistent performance.

A notable achievement was repurposing a pressure sensor to directly measure and display real-time pressure, eliminating the need for a commercial monitor. This approach showcased the feasibility and effectiveness of integrating the pressure sensor into the tubing. However, a potential concern is the risk of leakage, which could be mitigated by adding a separate tube to securely connect the pressure sensor to the air passageway.

To further enhance the project's functionality, modifications to the code can be implemented for increased convenience and broader applicability. This would be particularly beneficial for testing blood pressure readings, as the sensor is currently configured for use with a commercially available blood pressure cuff.

Moving forward, our project encountered challenges in achieving accurate blood pressure readings with the model arm, primarily due to limited pressure changes within the arm for the cuff to detect. Addressing this issue requires filling the reservoir with a fluid denser than water but not significantly more viscous, with salt water being a potential candidate. This denser fluid would facilitate more discernible pressure variations within the model arm.

Furthermore, optimizing materials to better simulate physiological properties is crucial. Exploring alternative materials for the rubber tube or silicone that closely match the mechanical and fluidic characteristics of human tissue can refine the model's accuracy and performance. Selecting materials with similar elasticity, compliance, and fluid behavior as human arteries can lead to more realistic blood pressure responses and improved measurement outcomes.

6.0 Broader Impact

Our work greatly impacts patients, with around half of the US population suffering from hypertension and therefore, requiring frequent blood pressure measurements to monitor the condition. The importance of developing a slim-cuff blood pressure monitor extends beyond patient monitoring.

6.1 Societal and Global Impact

The societal impact of our work is clear, as the slim cuff design can be integrated into shirt sleeves, making frequent blood pressure measurements more comfortable for the elderly

and less disruptive to patient routines. Many elderly patients, especially those with dementia, find it highly uncomfortable to have a bulky cuff wrapped around their arm multiple times a day for blood pressure monitoring. Additionally, the current cuff design requires high pressures and long wait times for accurate readings. The slim cuff, with its smaller profile and lower pressure requirements, will achieve accurate readings more quickly. This will significantly reduce patient discomfort and disruption, leading to increased patient satisfaction.

6.2 Engineering Ethics

The engineering ethics of our work are demonstrated by validating an anatomically and physiologically accurate arm simulator, eliminating the initial need for testing slim cuffs on human subjects. This simulator prioritizes patient safety, health, and welfare, streamlining the testing of slim cuff technology. Once validated, the slim cuff will offer a more comfortable and less disruptive option for blood pressure measurements, especially for patients who refuse the bulky cuff. This advancement will lead to improved patient satisfaction due to reduced pressure and wait times for accurate readings. Additionally, our partnership with Massachusetts General Hospital ensures the adherence to engineering ethics standards in advancing this technology.

6.3 Environmental Impact

This project involves manufacturing practices that impact the environment in the following two areas: 3D printing the silicone mold and casting the silicone model arm. Both PLA and silicone are not the most environmentally friendly materials because neither material can be recycled or degraded easily. PLA was chosen as the material for the silicone mold because it is cost and time-effective, both of which were important factors to consider in the limited time and budget allotted for this project. Additionally, PLA can be readily 3D printed, and 3D printing the silicone cast allowed for ease in modifications. Silicone was chosen as the primary material for the model arm because its material properties most closely aligned with the researched values for a human arm according to the literature. This choice, however, was also capped by available technologies and budget and time constraints. It is necessary to manufacture only one model arm, so investing more money to utilize more advanced and expensive technologies for the creation of this arm can be of benefit. Additionally, using a more environmentally friendly material and

manufacturing technique to create the model arm will eliminate the need to 3D print a PLA silicone mold.

6.4 Codes and Standards

While we did not employ technical codes and standards in the development of the arm simulator, the slim cuff design will undergo extensive testing according to codes and standards to ensure patient safety and accurate results. Currently, there is a standard for blood pressure cuff length and width in the industry; once the slim-cuff design is validated, new industry standards will be developed that reflect the novel slim-cuff technology. Additionally, the slim cuff technology will pass the Food and Drug Administration (FDA) standards prior to its introduction to healthcare systems, including the applicable requirements stated in ISO 81060. Specific requirements for calibration to ensure consistent accuracy will also be developed.

6.5 Economic Factors

Consumer cost is a major consideration when designing a novel product. The slim cuff technology, when validated and introduced into the industry, will be provided to the consumer at a cost similar to that of the traditional blood pressure cuff on the market today. Thus, the slim cuff technology will be widely accessible. Major stakeholders include hospitals, assisted living centers, patients, especially those with hypertension, and healthcare professionals. These stakeholders currently purchase the standard blood pressure cuff. When the slim cuff technology is introduced to the market, the advantageous benefits of patient comfort, wearability, low pressures, low wait times, and accurate readings will outweigh the slight cost advantage of the current industry standard cuff if the slim cuff technology is more costly.

References

Berger A. (2001). Oscillatory Blood Pressure Monitoring Devices. *BMJ : British Medical Journal*, *323*(7318), 919.

Centers for Disease Control and Prevention. (2023, July 6). *Facts about hypertension*. Centers for Disease Control and Prevention. https://www.cdc.gov/bloodpressure/facts.htm#:~:text=In%202021%2C%20hypertension%20was%20a,deaths%20in%20the%20United%20States.&text=Nearly%20half%20of%20adults%20have,are%20taking%20medication%20for%20hypertension%20Elliott%20W.%20J.%20(2003).%20The%20economic%20impact%20of%20hypertensio

Chung, E., Chen, G., Alexander, B., & Cannesson, M. (2013). Non-invasive continuous blood pressure monitoring: A review of current applications. *Frontiers of Medicine*, *7*(1), 91–101. https://doi.org/10.1007/s11684-013-0239-5

Grand View Research. (n.d.). Blood Pressure Monitoring Devices Market Size Report, 2030. https://www.grandviewresearch.com/industry-analysis/blood-pressure-monitoring-devices-market

Homan, T. D. (2023, July 10). *Physiology, pulse pressure*. StatPearls [Internet]. https://www.ncbi.nlm.nih.gov/books/NBK482408/#:~:text=Pulse%20pressure%20is%20the%20difference,Blood%20Pressure%20%E2%80%93%20Diastolic%20Blood%20Pressure

Khan, M. A., Gul, H., & Mansor Nizami, S. (n.d.). Determination of Gender from Various Measurements of the Humerus. *Cureus*, *12*(1), e6598. https://doi.org/10.7759/cureus.6598

Kumar, S., Yadav, S., & Kumar, A. (2022). Oscillometric Waveform Evaluation for Blood Pressure Devices. *Biomedical Engineering Advances*, *4*, 100046. https://doi.org/10.1016/j.bea.2022.100046

Lan, H., Al-Jumaily, A. M., Lowe, A., & Hing, W. (2011). Effect of tissue mechanical properties on cuff-based blood pressure measurements. *Medical Engineering & Physics*, *33*(10), 1287–1292. https://doi.org/10.1016/j.medengphy.2011.06.006

Leguy, C. A. D., Bosboom, E. M. H., Gelderblom, H., Hoeks, A. P. G., & van de Vosse, F. N. (2010). Estimation of distributed arterial mechanical properties using a wave propagation model in a

reverse way. *Medical Engineering & Physics*, *32*(9), 957–967. https://doi.org/10.1016/j.medengphy.2010.06.010

Natural Rubber. Designerdata. (n.d.). https://designerdata.nl/materials/natural-rubber

Rader, F., & Victor, R. G. (2017b). The slow evolution of blood pressure monitoring. *JACC: Basic to Translational Science*, *2*(6), 643–645. https://doi.org/10.1016/j.jacbts.2017.11.001

Roguin, A. (2005). Scipione Riva-Rocci and the men behind the Mercury Sphygmomanometer. *International Journal of Clinical Practice*, *60*(1), 73–79. https://doi.org/10.1111/j.1742-1241.2005.00548.x

Saugel, B., & Sessler, D. I. (2021). Perioperative Blood Pressure Management. *Anesthesiology*, *134*(2), 250–261. https://doi.org/10.1097/ALN.0000000000003610

Science Museum Group. (n.d.). *Hill and barnard-type sphygmomanometer, London, England, 1891-1900: Science Museum Group Collection*. Hill and Barnard-type sphygmomanometer, London, England, 1891-1900 | Science Museum Group. https://collection.sciencemuseumgroup.org.uk/objects/co93671/hill-and-barnard-type-sphygmomanometer-london-england-1891-1900-sphygmomanometer

Sparks, J. L., Vavalle, N. A., Kasting, K. E., Long, B., Tanaka, M. L., Sanger, P. A., Schnell, K., & Conner-Kerr, T. A. (2015). Use of silicone materials to simulate tissue biomechanics as related to deep tissue injury. *Advances in Skin & Wound Care*, *28*(2), 59–68. https://doi.org/10.1097/01.asw.0000460127.47415.6e

Appendices

Appendix A: Dimensioned CAD Drawings of Silicone Cast

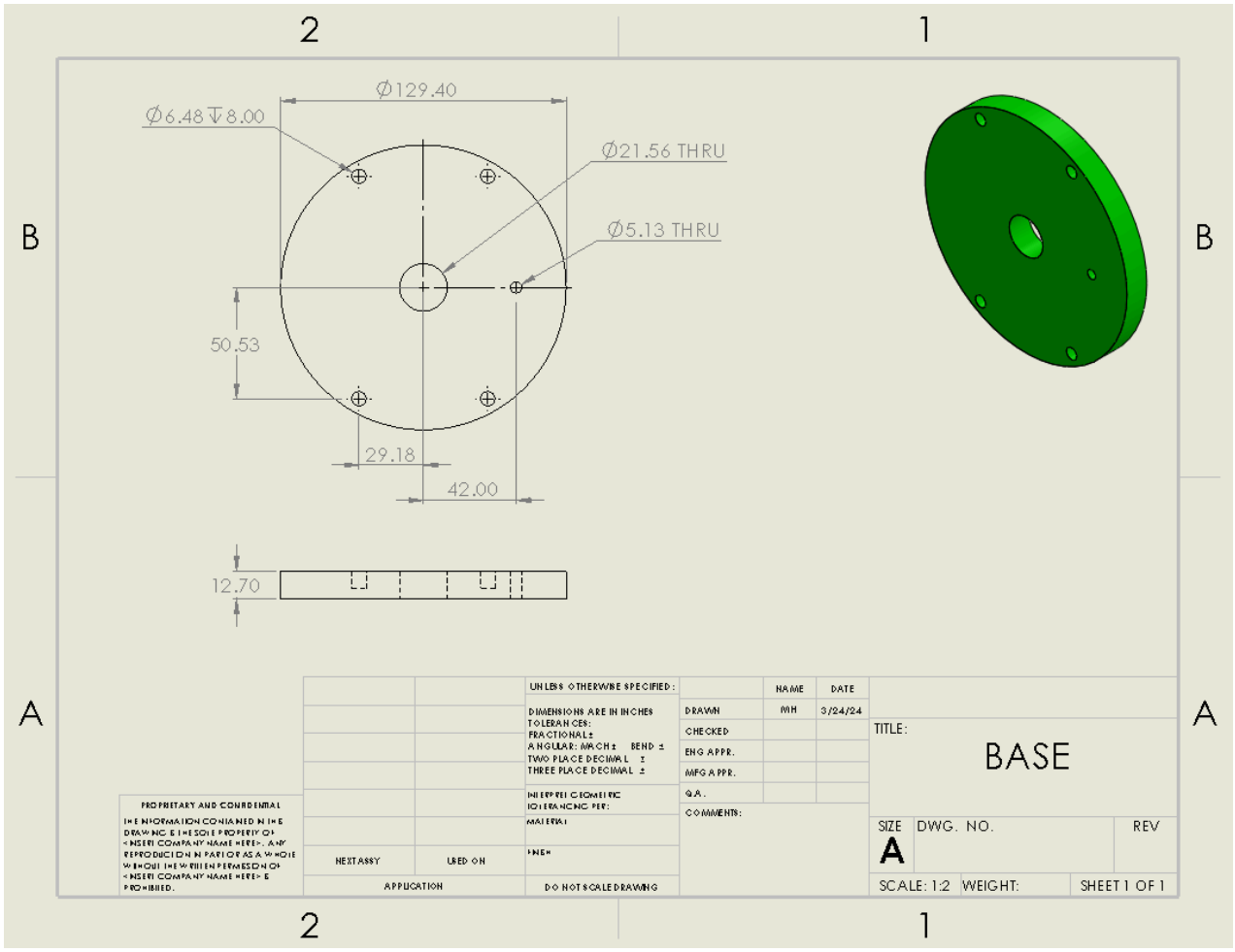

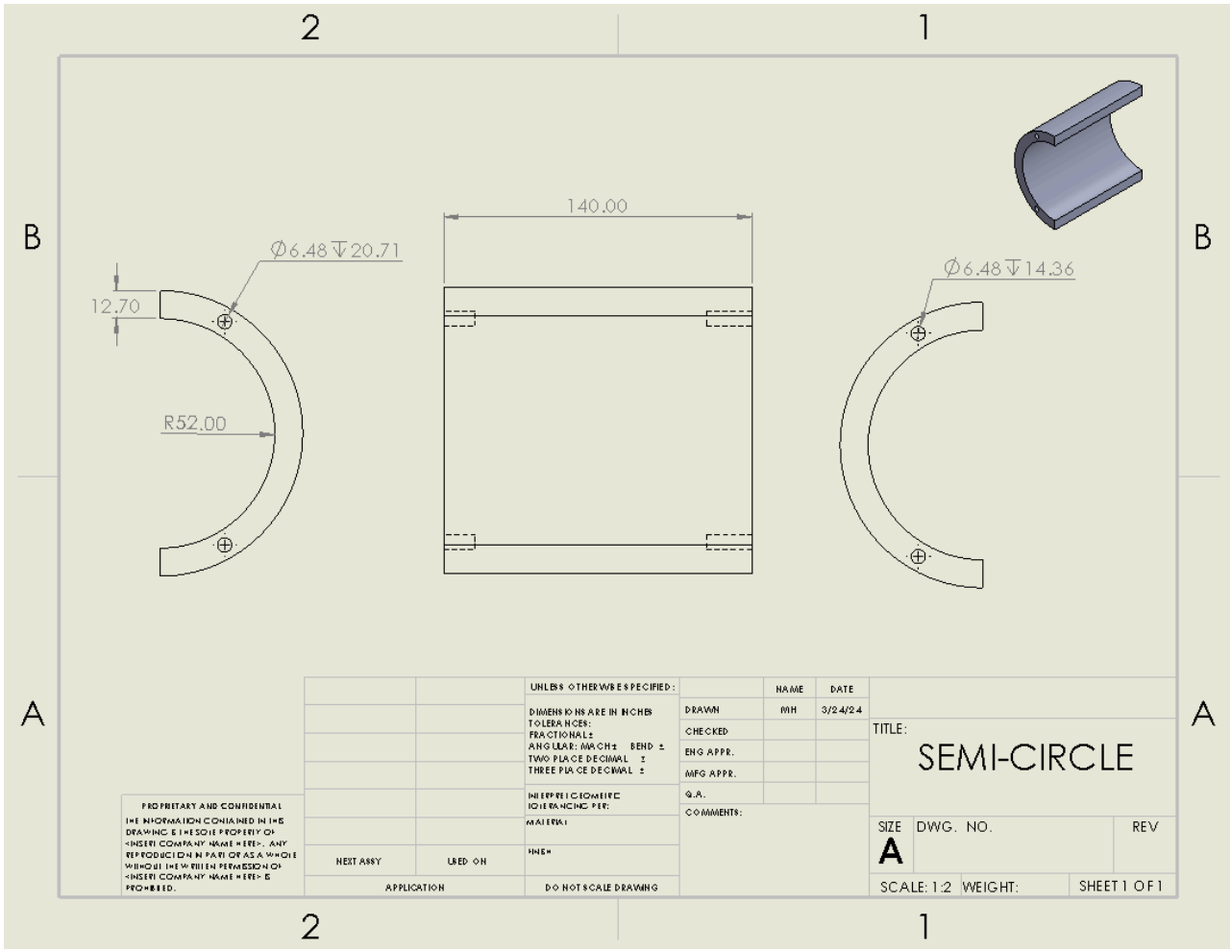
2
1
B
A
140.00
Ø6.48↧20.71
12.70
R52.00
Ø6.48↧14.36
UNLESS OTHERWISE SPECIFIED:
DIMENSIONS ARE IN INCHES
TOLERANCES:
FRACTIONAL ±
ANGULAR: MACH ± BEND ±
TWO PLACE DECIMAL ±
THREE PLACE DECIMAL ±
INTERPRET GEOMETRIC TOLERANCING PER:
MATERIAL
FINISH
NEXT ASSY
USED ON
APPLICATION
DO NOT SCALE DRAWING
NAME
DATE
DRAWN
MH
3/24/24
CHECKED
ENG APPR.
MFG APPR.
Q.A.
COMMENTS:
TITLE:
SEMI-CIRCLE
SIZE
A
DWG. NO.
REV
SCALE: 1:2
WEIGHT:
SHEET 1 OF 1
PROPRIETARY AND CONFIDENTIAL
THE INFORMATION CONTAINED IN THIS DRAWING IS THE SOLE PROPERTY OF <INSERT COMPANY NAME HERE>. ANY REPRODUCTION IN PART OR AS A WHOLE WITHOUT THE WRITTEN PERMISSION OF <INSERT COMPANY NAME HERE> IS PROHIBITED.

Appendix B: Arduino IDE Stepper Motor Code

```
#include <AccelStepper.h>

// Define some steppers and the pins it will use
AccelStepper stepper1(AccelStepper::DRIVER, 4, 7); //AccelStepper(DRIVER, STEP, DIR)
int flag;
int target_location;

void setup()
{
  stepper1.setPinsInverted(true);
  stepper1.setMaxSpeed(2700); // What max speed you want to move
  stepper1.setAcceleration(20000); // What max acceleration you want

  // stepper1.setSpeed(1500*2); // This is the set speed

  flag = 1;
  target_location = 1352;


  stepper1.moveTo(target_location); // How much you want to move //1352 steps = 500 mm
}

void loop()
{
  // Change direction at the limits
  if(stepper1.distanceToGo() == 0) {
    if(flag == 1){
      stepper1.moveTo(0);
      flag = 0;
    }else{
      stepper1.moveTo(target_location);
      flag = 1;
    }
  }
  stepper1.run();
}
```

Appendix C: Arduino Code for Data Acquisition System

```
#include "HX711.h"

const int LOADCELL_DOUT_PIN = 3;
const int LOADCELL_SCK_PIN = 2;
const int PUMP = 9;
const int VALVE = 4;
static  int hasRun = 0;
```

```
unsigned long startTime;
float pressure;
bool pumpON;
HX711 scale;

//---------------------------------------------------------------------

void setup() {
  Serial.begin(115200);
  pinMode(PUMP, OUTPUT);
  pinMode(VALVE, OUTPUT);
  startTime = millis();
  scale.begin(LOADCELL_DOUT_PIN, LOADCELL_SCK_PIN);
  scale.set_gain(128);
  //delay(5000);
}
//---------------------------------------------------------------------
void loop() {
  if (scale.is_ready()) {
    unsigned long currentTime = millis();
    unsigned long elapsedTime = currentTime - startTime;
    pressure = scale.read();

    float mv = (((5000/(pow(2,24)-1))*pressure/128)-.02328);
    float realPressure = (mv-0.2088)/0.0769;
    //Serial.print(elapsedTime);
    //Serial.print(',');
    Serial.println(realPressure);
    if (hasRun <1) {
      if (realPressure < 230){
        digitalWrite(PUMP, HIGH);      // consider switching to analog,
between 0-255
        digitalWrite(VALVE, HIGH);
        pumpON = true;
      }
      else if (pressure >= 230){
        analogWrite(PUMP, 0);
        digitalWrite(VALVE, HIGH);
        hasRun++;
      }
```

```
    }
 }
}
```

Appendix D: MATLAB Code for Pressure Calculations

```
%% Read Data from Arduino-----------------------------------------------------
clear;clc;
serialPort = 'COM4'; % '/dev/tty.usbserial-1440';
baudRate = 115200;
s =serial(serialPort,'BaudRate',baudRate); % Setting Up serial port
fopen(s);
numSamples = 2000;
data = zeros(1,numSamples);
tic
try
   for i = 1:numSamples
       serialData = fscanf(s,'%f');
       data(i) = serialData;
       disp(serialData)
   end
catch e
   disp('An error Occured')
   disp(e.message)
end
toc
fclose(s);
delete(s);
clear s;
save('0211Test','data')
%save('data2.mat',data)
%% Processing
Y = data;
X = 1:length(data);
[~,index] = max(Y); % Identifying peak of Y, to separate deflation curve
ind = index; % Start logging deflation curve after 2 seconds
```

```
y2 = Y(ind:end); % Stop logging deflation curve 2 seconds before the data
x2 = X(ind:end); % collection ends
lowerLimit =35;
if lowerLimit< Y(end)
   lowerLimit = Y(end-80);
end
[~,P1] = find(y2<=155);
[~,P2] = find(y2<lowerLimit);
Y2 = y2(P1(1):P2(1));
X2 = x2(P1(1):P2(1));
Fs = 40; % Sampling frequency in Hz (adjust this according to your data)
tDeflate = length(Y2)/Fs; % Return Deflation time
% Print Estimate Deflation time
fprintf('The deflation time is %.2f seconds \n',tDeflate) %Print Estimate
Deflation time
%% GPT Bandpass Filter
% Define the filter specifications
low_cutoff = 0.9;   % Lower cutoff frequency in Hz
high_cutoff = 3;   % Upper cutoff frequency in Hz
% Determine the filter order and cutoff frequencies
Wp = [low_cutoff high_cutoff]/(Fs/2);
Ws = [0.05 5.45]/(Fs/2);
Rp = 3;
Rs = 5;
[n,Wn] = buttord(Wp,Ws,Rp,Rs);
% Design the Butterworth bandpass filter
[b, a] = butter(n, Wn, 'bandpass');
% Apply the filter to your signal (replace 'signal' with your actual data)
filtered = filtfilt(b, a, Y2);
%% Finding Peaks for filtered data, Prepare OMW
%OMW = filtered'-lower;
%invOMW = -1*OMW;
% pUP = Upper Peak value
% ind_pUP = index of upper peak
% ind_pLOW = index of lower peak
favg = mean(abs(filtered))*0.5;
invfilt = -1*filtered; % Need to invert the signal for lower peak
identification
```

```
[fUP,ind_fUP] =
findpeaks(filtered,'MinPeakProminence',favg,'MinPeakDistance',20);
[inv_pLOW,ind_pLOW] = findpeaks(invfilt,'MinPeakDistance',20);
pLOW = -1*inv_pLOW;
fup = interp1(X2(ind_fUP),fUP,X2,'pchip'); % Upper envelope
down = interp1(X2(ind_pLOW),pLOW,X2,'pchip'); % Lower envelope
cut = ind_pLOW(2);
%---------------- MoD---------------
fup = fup(cut:end);
down1 = down(cut:end);
down2 = down(cut:end);
envX = X2(cut:end);
OMW2 = filtered(cut:end)-down2;
envX2 = X2(cut:end);
% Getting  OMW
OMW = fup-down1; % Needs polyfit to refine
%[~,indOMW] = min(OMW);
%OMW = OMW(indOMW:end);
%X3 = X2(indOMW:end);
%% PLOTs
[p2,~,mu2] = polyfit(envX,OMW,9);
omw_poly = polyval(p2,envX,[],mu2);
multi = 50;
%% BP Cal
a = omw_poly;
b = Y2(cut:end);
[aABP,ABPLOC] = max(a);
%mybar = (max(Y2)-min(Y2))/length(Y2);
mybar = 0.025;
aSBP = 0.3*aABP;
SBP_TEMP = find((a < aSBP+mybar) & (a > aSBP-mybar));
SBP_LOC = SBP_TEMP(SBP_TEMP < ABPLOC);
aDBP = 0.9*aABP;
DBP_TEMP = find((a < aDBP+mybar) & (a > aDBP-mybar));
DBP_LOC = DBP_TEMP(DBP_TEMP > ABPLOC);
sbp = mean(b(SBP_LOC));
dbp = mean(b(DBP_LOC));
MAP = b(ABPLOC);
```

```
pp = sbp-dbp;
fprintf('The SBP,DBP,MAP from OMW1 are %.2f,%.2f,%.2f \n',sbp,dbp,MAP)
%% Raw Data and Deflation Curve Plot
figure
plot(X,Y,'b',X2,Y2,'r')
xlabel('Time (ms)');
ylabel('mmHg');
legend('Raw Data','Deflation Curve')
title('Raw Data')
%% Filtered Peaks and Envelope, with OMW
figure
subplot(2,1,1)
plot(envX,filtered(cut:end),'k',envX,fup,'r',envX,down1,'g')
hold on
scatter(X2(ind_pLOW),pLOW,'gx')
hold off
title('Envelope')
xlabel('Real Time')
ylabel('Magnitude')
legend('Filtered','Upper Envelope','Lower Envelope','Upper peaks','Lower
peaks')
subplot(2,1,2)
plot(envX,OMW,'k',envX,omw_poly)
title('OMW')
xlabel('Real Time')
ylabel('Amplitude')
legend('OMW','OMW_POLY')
%% Range for OMW BP Cal
figure
hold on
plot(envX,omw_poly*multi,'r',envX,b,'k')
scatter(envX(SBP_LOC),b(SBP_LOC),'bx')
scatter(envX(DBP_LOC),b(DBP_LOC),'gx')
scatter(envX(ABPLOC),b(ABPLOC),'bo')
scatter(envX(ABPLOC),aABP*multi,'ro')
xlabel('Time')
ylabel('mmHg')
title('Range for SBP/DBP Cal')
```

```
legend('OMW Curve','Deflation Curve','SBP points','DBP points','ABP on
Deflation curve','ABP on OMW')
%%
figure
plot(OMW2)
%%End------------------------------------------------------------------------
```